

Modeling Dynamic Seismic Responses in Isolators via Advanced Numerical Methods

Alessandro Bianchi, Elena Maria Fabbri

Department of Civil Engineering, University of Bologna, Italy / Department of Structural Engineering, Politecnico di Milano, Italy

Abstract—In this paper, a one-dimensional (1d) Parallel ElastoPlastic Model (PEPM), able to simulate the uniaxial dynamic behavior of seismic isolators having a continuously decreasing tangent stiffness with increasing displacement, is presented. The parallel modeling concept is applied to discretize the continuously decreasing tangent stiffness function, thus allowing to simulate the dynamic behavior of seismic isolation bearings by putting linear elastic and nonlinear elastic-perfectly plastic elements in parallel. The mathematical model has been validated by comparing the experimental force-displacement hysteresis loops, obtained testing a helical wire rope isolator and a recycled rubber-fiber reinforced bearing, with those predicted numerically. Good agreement between the simulated and experimental results shows that the proposed model can be an effective numerical tool to predict the force-displacement relationship of seismic isolators within relatively large displacements. Compared to the widely used Bouc-Wen model, the proposed one allows to avoid the numerical solution of a first order ordinary nonlinear differential equation for each time step of a nonlinear time history analysis, thus reducing the computation effort, and requires the evaluation of only three model parameters from experimental tests, namely the initial tangent stiffness, the asymptotic tangent stiffness, and a parameter defining the transition from the initial to the asymptotic tangent stiffness.

I. INTRODUCTION

B

ASE isolation is a seismic design method that allows to reduce transmission of horizontal ground movement into the structure by introducing a flexible base isolation system, generally consisting of seismic isolators and a full diaphragm above the isolation devices, between the foundation and the superstructure [1], [2]. Seismic isolators can be divided into two main categories: elastomeric-based or sliding-based bearings. The former rely on the flexibility of rubber to achieve isolation, whereas the latter allow to achieve low horizontal stiffness through the action of sliding and to dissipate energy through the friction damping occurring at the sliding interface [3].

Metal devices, such as wire rope isolators, currently used for the seismic protection of equipment in buildings [4], can be adopted with flat or curved surface sliders when the complete recentering of the baseisolated structure is required and when the displacements of

the base isolation system have to be reduced [5].

The above-mentioned seismic devices generally exhibit symmetric softening force-displacement hysteresis loops under design dynamic loading [3]. Models with bilinear characteristics can represent the dynamic behavior of elastomeric-based bearings and wire rope isolators, whereas models with rigid-plastic characteristics can be adopted to simulate the dynamic response of sliding-based bearings. The Bouc-Wen Model (BWM) has been adapted for modeling the uniaxial behavior of both elastomeric and sliding bearings and wire rope isolators [4], [6].

In this work, a 1d PEPM is presented in order to avoid the numerical solution of the first order ordinary nonlinear differential equation required in the BWM, and to reduce the number of model parameters to be identified from experimental tests. The proposed nonlinear hysteretic model stems from the hypothesis that the tangent horizontal stiffness exponentially decreases with increasing displacement within relatively large displacements. Hysteretic curves with continuously decreasing stiffness can be easily discretized using the parallel modeling concept. The basic idea is to consider one purely linear elastic element and a sufficiently high number of simple nonlinear elastic-perfectly plastic elements connected in parallel, all having the same deformation but each carrying a different force, and to calculate the total restoring force of the parallel assemblage by summing the forces acting on each element.

Parallel modeling has been already used in the past for representing the mechanical behavior of inelastic materials. The idea of effective stress introduced by Terzaghi to describe the behavior of wet soils is essentially a parallel model, as water and soil fabric both carry the total stress. The concept was first formalized by [7] in treating non-associated flow plasticity and then used by [8], [9] to achieve a better representation of actual material behavior through a number of overlays of simple models. Nelson and Dorfmann [10] have used parallel models in incremental elasto-plasticity to represent strain hardening in metals and to develop models of frictional materials such as soils, rock and concrete.

The proposed model requires the evaluation of only three parameters, namely, the initial and asymptotic tangent

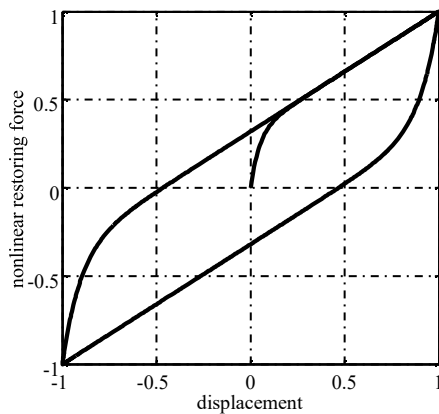


stiffnesses, and a parameter defining the transition from the initial to the asymptotic tangent stiffness, whereas the widely used BWM requires seven parameters to be identified for modeling the dynamic behavior of elastomeric bearings, flat sliding bearings and wire rope isolators [4], [11].

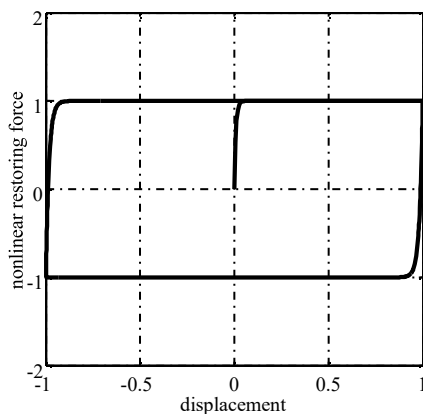
The mathematical model has been validated by comparing the experimental hysteresis loops obtained during cyclic tests, conducted on a helical wire rope isolator and a recycled rubber-fiber reinforced bearing at the Department of Industrial Engineering of the University of Naples Federico II, with those predicted numerically.

II. DYNAMIC BEHAVIOR OF ISOLATORS UNDER DESIGN LOAD

Seismic isolators generally exhibit symmetric softening force-displacement hysteresis loops under design dynamic loading. More specifically, elastomeric bearings, such as high damping rubber bearings and lead rubber bearings, and metal devices, such as wire rope isolators, show a force displacement loop with bilinear characteristics (Fig. 1 (a)), whereas sliding bearings, such as flat sliding bearings, display hysteresis loops having rigid-plastic characteristics (Fig. 1 (b)).



(a)



(b)

Fig. 1 Normalized force-displacement loop having (a) bilinear and (b) rigid-plastic characteristics

In both two cases, the tangent horizontal stiffness exponentially decreases with increasing displacement from an initial value to an asymptotic value. Thus, the tangent stiffness $k_t(u)$ can be expressed by the following two mathematical expressions, valid for a loading and an unloading curve, respectively:

$$k_t(u) = k_0 - (k_0 - k_\infty) e^{-c(u - u_{min})}, \quad (u \geq 0) \quad (1)$$

$$k_t(u) = k_0 - (k_0 - k_\infty) e^{-c(u_{max} - u)}, \quad (u \leq 0) \quad (2)$$

where k_0 and k_∞ are the initial and the asymptotic values of the tangent stiffness, u_{max} and u_{min} are the displacement values at the most recent point of unloading and loading, respectively, and c is a parameter that defines the transition from k_0 to k_∞ .

III. PARALLEL MODELING OF INELASTIC MATERIAL BEHAVIOR

Hysteretic curves with continuously decreasing tangent stiffness, like those shown in the previous section, can be easily discretized using the parallel modeling concept. The basic idea is to consider purely elastic elements and elastic perfectly plastic elements connected in parallel, all having the same deformation but each carrying a different force. The total force acting on the parallel assemblage can be obtained by summing the forces acting on each element.

Fig. 2 shows a 1d stress-strain curve for a work hardening material which is elastic with Young's modulus E up to a yield stress σ_y and then presents a tangent stiffness $E_t \ll E$ above the yield stress. The material is assumed to have the same yield stress in compression as in tension and to exhibit kinematic hardening, that is, the difference between the stresses which limit the elastic range remains constant during cyclic loading.

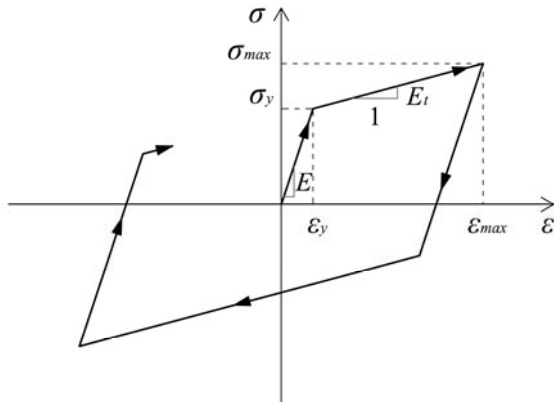


Fig. 2 Stress-strain curve for a work hardening material

The above-described 1d stress-strain curve can be reproduced by adopting a two-element parallel model (Fig. 3), obtained by putting in parallel an elastic element with Young’s modulus E_t and an elastic-perfectly plastic element having elastic stiffness $E \ll E_t$ and a yield stress $(1 \ll E_t/E) \sigma_y$.

It is important to note that the parallel model does not only reproduce the stress-strain curve during the loading, but also the behavior during unloading and cyclic loops as well as kinematic hardening.

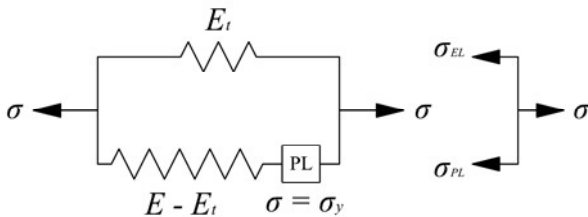


Fig. 3 Schematic diagram of a two-element parallel model

The previous simple two-element model can be easily generalized to the case of a multilinear 1d stress-strain curve, using one elastic element and a finite number of elastic-perfectly plastic elements connected in parallel. As shown in Fig. 4 for the case of a total of four constitutive elements, the initial stiffness of the parallel assemblage is the sum of the elastic stiffness of each element. As the carried load increases, each of the elasto-plastic elements yields and the total stiffness correspondingly decreases.

It is easy to understand that 1d curves with continuously decreasing stiffness, like those exhibited by isolation bearings, can be effectively approximated through parallel modeling using a sufficiently high number of constitutive elements.

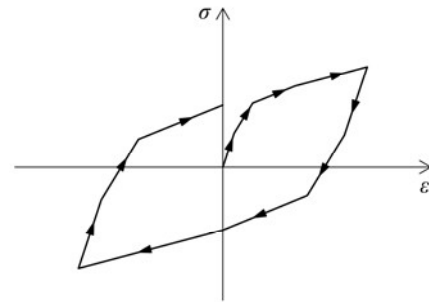


Fig. 4 Stress-strain curve obtained using a four-element parallel model

IV. APPLICATION OF PARALLEL MODELING TO SEISMIC ISOLATORS

In this section, a 1d PEPM is proposed to simulate the dynamic behavior of seismic isolators within a relatively large displacements range, generally reached under the design loading.

The continuously decreasing tangent stiffness of a seismic isolator can be expressed by:

$$k_t(u) \approx k_0 \left[1 - a e^{-cu} \right], \quad (3)$$

valid for a generic loading or unloading curve obtained during cyclic testing on a single isolation bearing, where $a \approx k_0 \ll k_0$, and u is evaluated starting from the latest point of unloading or reloading.

According to Masing rules, the first loading curve, namely the virgin curve, can be obtained from the generic loading or unloading curve from a similitude transformation of ratio 0.5. This means that for a given u on the virgin curve, where u is computed starting from zero, the corresponding tangent stiffness must be equal to the one obtained from the generic loading or unloading curve for a value of $2u$. Thus, in order to obtain the tangent stiffness for the virgin curve, it is just necessary to substitute c with $2c$ in (3):

$$k_t(u) \approx k_0 \left[1 - a e^{-2cu} \right]. \quad (4)$$

The continuously decreasing tangent stiffness function relative to the virgin curve can be approximated through a piecewise constant function with $N + 1$ equally spaced decreasing values of $k_t(u)$, as shown in Fig. 5.

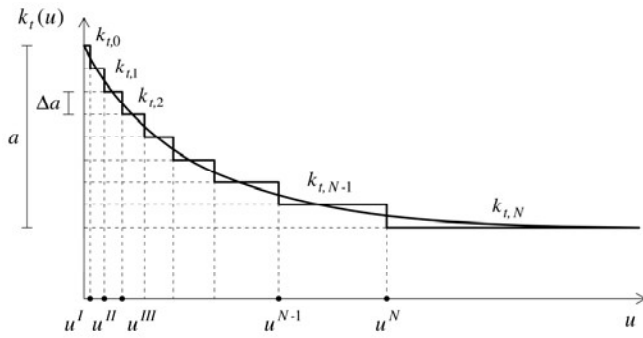


Fig. 5 Continuous and discretized tangent stiffness for the virgin curve

Assuming $\Delta a = a/N$, the discretized tangent stiffness values are:

$$k_{t,0} = k_0 - \alpha a, \tag{5}$$

$$k_{t,1} = k_0 - (N-1)\Delta a, \tag{6}$$

$$k_{t,2} = k_0 - (N-2)\Delta a, \tag{7}$$

$$k_{t,N-1} = k_0 - \Delta a, \tag{8}$$

$$k_{t,N} = k_0, \tag{9}$$

and the corresponding values of the displacements are obtained by solving (4) with respect to u :

$$u_j = \frac{1}{2c} \left[\log \left(\frac{k_{t,j} - k_0}{k_{t,j} - \alpha} \right) + \frac{1}{\alpha} \right] \quad j = 0, 1, \dots, N-1. \tag{10}$$

Once the $(u_j, k_{t,j})$ points have been determined, the expression of the tangent stiffness for the virgin curve can be approximated through the piecewise constant function given by:

$$u = u^I = k_t(u) = k_{t,0} = k_0 - \alpha a, \tag{11}$$

$$u^I = u = u^{II} = k_t(u) = k_{t,1}, \tag{12}$$

$$u^{II} = u = u^{III} = k_t(u) = k_{t,2}, \tag{13}$$

$$u_{N-1} = u = u_N = k_t(u) = k_{t,N-1}, \tag{14}$$

$$u = u^N = k_t(u) = k_{t,N} = k_0, \tag{15}$$

where the limit displacement values u^i are:

$$u^I = \frac{u_0 + u_1}{2}, \tag{16}$$

$$u^{II} = \frac{u_1 + u_2}{2}, \tag{17}$$

$$u_{N-1} = \frac{u_{N-2} + u_{N-1}}{2}, \tag{18}$$

$$u_N = \alpha u_{N-1}, \tag{19}$$

and α is an appropriate constant.

A single seismic isolator can be represented by parallel assemblage of one 1d elastic element of stiffness $k_{el} = k_0$ and N 1d elastic-perfectly plastic elements having stiffness $k_{ep,i} = \alpha a$ when in the elastic state and yielding displacement

u_i , for $i = I, II, \dots, N$.

Compared to the widely used BWM, the proposed PEPM does not require the solution of a first order ordinary nonlinear ordinary differential equation for each time step of a nonlinear time history analysis, thus allowing to reduce the computational effort. Furthermore, the PEPM requires the evaluation of only three parameters, namely, the initial tangent stiffness, the asymptotic tangent stiffness, and a parameter defining the transition from the initial to the asymptotic tangent stiffness, whereas the BWM requires seven parameters to be identified for modeling the dynamic behavior of elastomeric bearings, flat sliding bearings, and wire rope isolators.

V. COMPARISON BETWEEN NUMERICAL AND EXPERIMENTAL RESULTS

To demonstrate the validity of the proposed mathematical model, the results predicted adopting the PEPM are compared to the experimental ones obtained from horizontal dynamic tests carried out on two types of seismic isolators, the Helical Wire Rope Isolator (HWRI) and Recycled Rubber-Fiber Reinforced Bearing (RR-FRB).

The adopted testing machine, available at the Department of Industrial Engineering of the University of Naples Federico II (Italy), is shown in Fig. 6. It consists of a sliding table driven by a horizontal hydraulic actuator,

powered by a 75 kW AC electric motor that allows to impose both displacement or load histories. The maximum horizontal force is about 50 kN, while the maximum speed is 2.2 m/s and the maximum stroke is ± 0.2 m. A vertical hydraulic actuator allows to apply a load up to 190 kN during tests. The experimental apparatus is instrumented in order to measure the relative horizontal displacement between the lower basement and the upper plate, the vertical load and the lateral load time histories [12]. All tests were conducted by imposing horizontal displacements at room temperature and the data were sampled at 250 Hz.

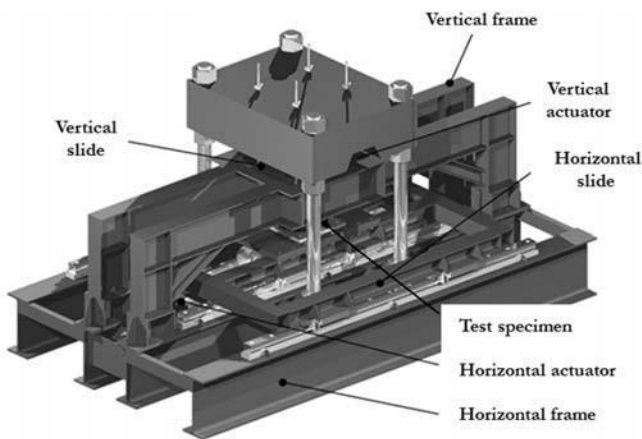


Fig. 6 Testing machine

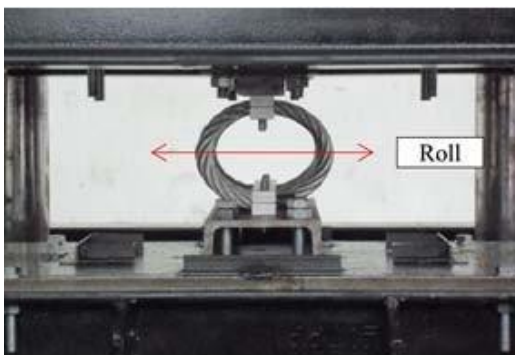
The tested HWRI, manufactured by Powerflex S.r.l (Limatola, Italy), is made of a wire rope, wound in the form of a helix and having diameter of 16 mm, and two slotted metal retainer bars in which the cable is embedded. The length, width, and height of the metal device are equal to 267 mm, 110 mm, and 100 mm, respectively. Fig. 7 shows the selected HWRI and its two principal horizontal directions, namely, Roll and Shear directions.

Five cycles of sinusoidal displacement, having frequency $f = 1$ Hz, were applied in both two main horizontal directions without the effect of the vertical load, for two different values of amplitude A , that is, 25 mm and 50 mm.

The tested RR-FRB (Fig. 8), manufactured by Isolgamma S.r.l. (Vicenza, Italy), consists of 12 layers of recycled rubber and 11 high strength quadridirectional carbon fiber fabric sheets, used as reinforcing elements. The bearing is square in plan, with dimensions 70 mm x 70 mm, and has a total height of approximately 63 mm. The carbon fiber layers have an equivalent thickness of 0.07 mm. The shear modulus of the recycled rubber, under the applied vertical load $P_v = 16.9$ kN, is equal to approximately 1 MPa at 100% shear strain [13].



Fig. 8 Tested RR-FRB



(a)

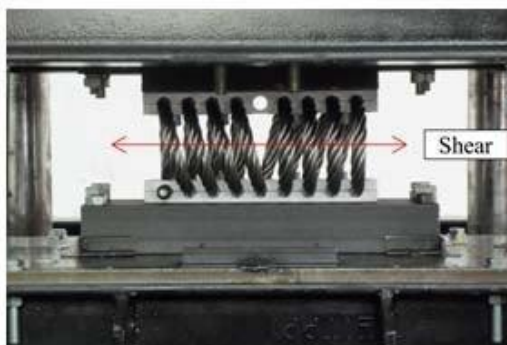


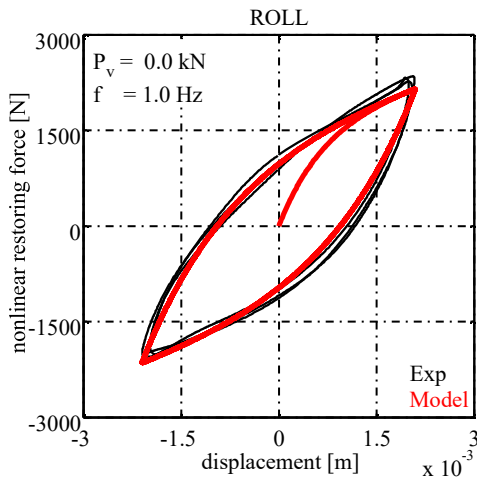
Fig. 7 Tested HWRI and its principal horizontal directions: (a) Roll and (b) Shear directions

The RR-FRB has been tested, using the above-described testing machine, in unbounded configuration, by imposing three cycles of harmonic displacement, having frequency $f = 0.87$ Hz, under the effect of a constant vertical pressure of 3.45 MPa, for two different values of amplitude A , namely 10 mm and 20 mm.

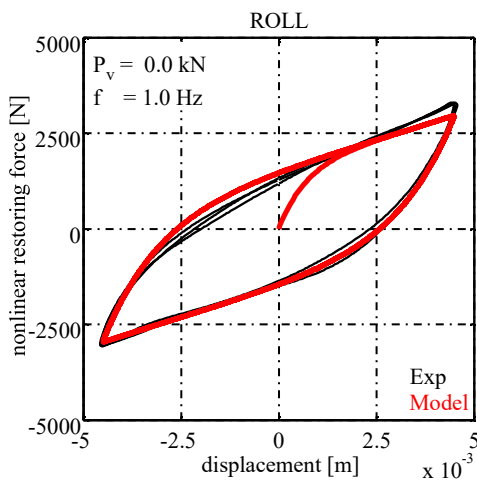
Figs. 9 (a) and (b) reveal the comparisons of the experimental and numerical results obtained in Roll direction for the HWRI under a test frequency of 1 Hz and a displacement amplitude equal to 25 mm and 50 mm, respectively. The total number of constitutive elements adopted in the PEPM is equal to 100. It can be observed that the agreement between the experimental and numerical responses is satisfactory.

Since the same good correlation between the experimental and numerical results has been obtained in Shear direction, these results are omitted for brevity.

It is worth to point out that experimental hysteresis forcedisplacement loops with different displacement amplitudes, like those shown in Fig. 10, can be satisfactorily represented by the proposed PEPM using only one set of three model parameters, that is, k_0 , k_{\square} , and c , determined from experimental loops with the largest amplitude.



(a)



(b)

Fig. 9 Comparisons of experimental and numerical results of HWRI in Roll direction: (a) $A = 25$ mm and (b) $A = 50$ mm

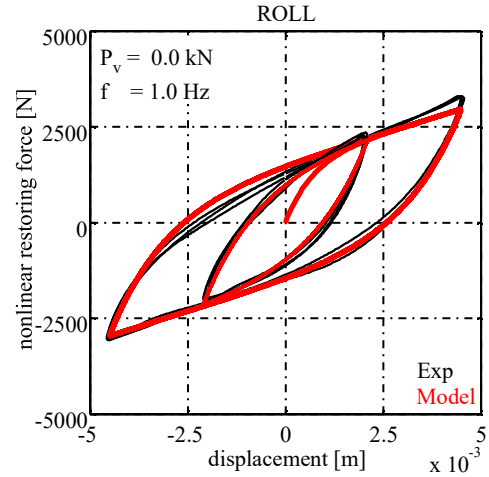
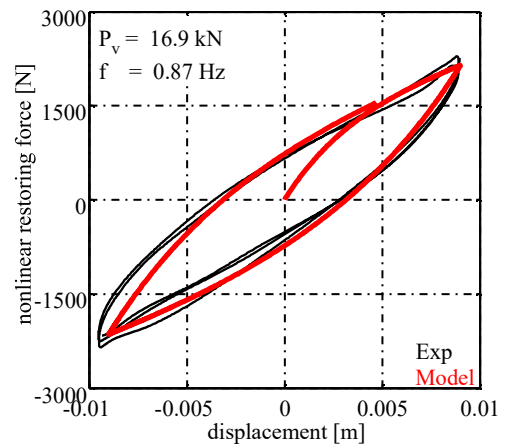


Fig. 10 Hysteresis loops with different amplitudes simulated using only one set of three model parameters

Finally, Figs. 10 (a) and (b) show the experimental and numerical hysteresis loops of RR-FRB obtained applying a sinusoidal harmonic motion having frequency of 0.87 Hz under the effect of a vertical load of 16.9 kN, for a displacement amplitude equal to 10 mm and 20 mm, respectively. It is evident that the proposed PEPM, adopting a total number of constitutive elements equal to 100, is capable of well-predicting the dynamic behavior of the tested device.



(a)

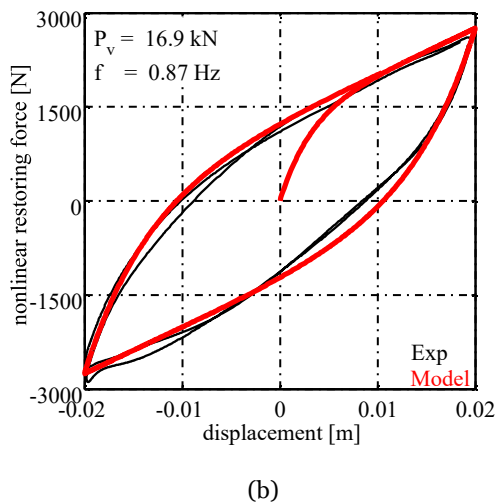


Fig. 11 Comparisons of experimental and numerical results of RFRB: (a) $A = 10$ mm and (b) $A = 20$ mm

VI. CONCLUSIONS

A 1d PEPM has been proposed to predict the dynamic behavior of seismic isolation bearings displaying symmetric softening force-displacement loops with bilinear characteristics, such as elastomeric bearings and wire rope isolators, or rigid-plastic characteristics, such as sliding bearings, within a relatively large displacements range, generally reached under the design dynamic loading. Assuming an exponentially decreasing tangent horizontal stiffness with increasing displacement, the force-displacement hysteresis loops have been simulated by putting in parallel one purely linear elastic element and a sufficiently high number of simple nonlinear elastic-perfectly plastic elements. In order to show the validity of the proposed mathematical model, the experimental hysteresis loops, obtained from cyclic dynamic tests performed on a HWRI and a RR-FRB, have been predicted by using the proposed PEPM. Good agreement between the experimental and numerical results was obtained. Compared to the widely used differential equation BWM, the proposed one does not require the numerical solution of a first order ordinary nonlinear differential equation for each time step of a nonlinear time history analysis, thus reducing the computation effort, and needs only three model parameters to be identified from experimental tests. Furthermore, the proposed PEPM is able to simulate hysteresis loops having different displacement amplitudes by adopting only one set of three model parameters determined from experimental loops with largest amplitude.

REFERENCES

- [1] J. M. Kelly, *Earthquake-resistant Design with Rubber*. London: Springer-Verlag, 1997.
- [2] F. Naeim and J. M. Kelly, *Design of Seismic Isolated Structures: From Theory to Practice*. New York: John Wiley & Sons, 1999.
- [3] M. C. Constantinou, A. S. Whittaker, Y. Kalpakidis, D. M. Fenz and G. P. Warn, "Performance of seismic isolation hardware under service and seismic loading," Technical Report MCEER-07-0012, State University of New York, Buffalo, 2007.
- [4] G. F. Demetriades, M. C. Constantinou and A. M. Reinhorn, "Study of wire rope systems for seismic protection of equipment in buildings," *Engineering Structures*, vol. 15, no. 5, pp. 321-334, 1993.
- [5] M. Spizzuoco, V. Quaglini, A. Calabrese, G. Serino and C. Zambrano, "Study of wire rope devices for improving the re-centering capability of base isolated buildings," *Structural Control and Health Monitoring*, to be published.
- [6] S. Nagarajaiah, A. M. Reinhorn and M. C. Constantinou, "Nonlinear dynamic analysis of 3-D base-isolated structures," *Journal of Structural Engineering*, vol. 117, no. 7, pp. 2035-2054, 1991.
- [7] A. Mroz, "Non-associated flow rules in plasticity," *Journal de Mecanique*, vol. 2, pp. 21-42, 1963.
- [8] D. R. J. Owen, A. Prakash and O. C. Zienkiewicz, "Finite element analysis of non-linear composite materials by use of overlay systems," *Computer and Structures*, vol. 4, pp. 1251-1267, 1974.
- [9] G. N. Pande, D. R. J. Owen and O. C. Zienkiewicz, "Overlay models in time-dependent nonlinear material analysis," *Computer and Structures*, vol. 7, pp. 435-443, 1977.
- [10] R. B. Nelson and A. Dorfmann, "Parallel elastoplastic models of inelastic material behavior," *Journal of Engineering Mechanics ASCE*, vol. 121, no. 10, pp. 1089-1097, 1995.
- [11] P. C. Tsopelas, P. C. Roussis, M. C. Constantinou, R. Buchanan and A. M. Reinhorn, "3D-BASIS-ME-MB: Computer program for nonlinear dynamic analysis of seismically isolated structures," Technical Report MCEER-05-0009, State University of New York, Buffalo, 2005.
- [12] S. Pagano, M. Russo, S. Strano and M. Terzo, "A mixed approach for the control of a testing equipment employed for earthquake isolation systems," *Journal of Mechanical Engineering Science*, vol. 228, no. 2, pp. 246-261, 2014.
- [13] M. Spizzuoco, A. Calabrese and G. Serino, "Innovative low-cost recycled rubber-fiber reinforced isolator: experimental tests and finite element analyses," *Engineering Structures*, vol. 76, pp. 99-111, 2014.